

**First-principles simulations of atomic networks and optical properties of amorphous SiN<sub>x</sub> alloys**

Fernando Alvarez and Ariel A. Valladares\*

*Instituto de Investigaciones en Materiales, UNAM, Apartado Postal 70-360, México DF 04510, México*

(Received 30 July 2002; revised manuscript received 14 August 2003; published 5 November 2003)

We report *ab initio* generated atomic networks of amorphous silicon-nitrogen alloys,  $a\text{-SiN}_x$ , for 13 different values of content  $x$  [from 0 to the nearly stoichiometric composition of  $x = (36/28) = 1.29$ ]. The amorphous structures were obtained using a new thermal procedure. 64-atom periodically continued cubic diamondlike cells, containing silicon and randomly substituted nitrogen, were amorphized by “heating” them to just below the corresponding melting temperatures, using a 6 fs time step and a Harris-functional based molecular dynamics code. After cooling, annealing, and optimizing, radial distribution functions (RDFs) and optical gaps were calculated for all samples. All the partial radial features obtained are new; the total RDF’s agree very well with the scarce experimental results. The electron energy levels were then calculated and the optical gaps obtained using a novel Tauc-like procedure that is not sensitive to gap states and band tails. The gap values agree with experiment.

DOI: 10.1103/PhysRevB.68.205203

PACS number(s): 71.23.Cq, 71.15.Pd, 71.55.Jv

**I. INTRODUCTION**

Simulating the atomic and electronic structure of amorphous semiconductors has proven to be a difficult task. Efforts have been pursued along two main lines: on the one hand the classical modeling of interatomic potentials that have permitted the study of large samples of pure elements, with thousands and millions of atoms;<sup>1,2</sup> on the other hand the quantum methods, parametrized<sup>3</sup> and *ab initio*, that aim at describing the systems without recourse to classical potentials that, by necessity, leave out interactions and correlations proper to the quantum entities that form the systems. Although both the classical and the parametrized quantum approaches arguably have the shortcoming of the nontransferability of the atomic potentials, they both are used when a more specific description is sought and the corresponding potentials are known. However, the *ab initio* techniques are the way to go whenever good qualitative universal results are required and whenever new parameters are needed for the above-mentioned approximate techniques.<sup>4</sup> Their shortcoming is the large computer resources needed to deal with cells of several hundred atoms that would make the description of the electronic and atomic structures of amorphous semiconductors more inclusive.

Amorphous SiN<sub>x</sub> alloys have attracted a great deal of attention in the last decades since they have electrical, optical, and mechanical features useful from the applicational viewpoint and their accentuated covalency makes them very interesting from the basic point of view. Nevertheless the experimental and theoretical knowledge of their atomic, electronic, and optical properties is not as ample as its importance merits. For example, experimentally their total radial distribution functions (RDF’s) are practically unknown, except for the stoichiometric composition, and the partial radial features are nonexistent. Theoretically, no *ab initio* attempt at simulating total and partial RDF’s has been performed, although first-principles studies of the electronic properties of previously *classically* generated (with Tersoff-like interatomic potentials) random structures have been reported recently.<sup>5</sup> Experimental studies have shown that their

optical gaps depend strongly on the nitrogen content  $x$  for  $0 \leq x \leq 1.33$  so they can be tuned to fit specific needs in solar cells. Some semiempirical studies have been done on their electronic structure, optical gaps and RDF’s and a first-principles approach has been used on an *ad hoc* constructed amorphous cluster structure. Since no first-principles attempt has been reported at simulating random networks, and therefore at simulating realistic total and partial RDF’s, any *ab initio* approach that adequately generates, describes, and predicts the atomic topology of  $a\text{-SiN}_x$  can be useful to understand their electronic features and can be applied to other covalent amorphous materials.

Precise *ab initio* calculations of optical gaps in crystalline semiconductors is a difficult problem. The common approximations used within density-functional theory (DFT) always underestimate these gaps; DFT is a ground-state theory and the transition of electrons to the conduction band cannot be adequately described. Nevertheless, recent attempts due to Louie and co-workers and Reining and her group, using Hedin’s many-body approach,<sup>6</sup> are promising. However, tackling realistic random networks with these techniques is not yet possible since the large number of atoms and the lack of symmetries in the amorphous cells make them computationally untractable at present. Moreover, in crystalline solids HOMO’s (highest occupied molecular orbitals) and LUMO’s (lowest unoccupied molecular orbitals) can be identified and a “gap,” equal to the difference LUMO-HOMO, may be defined. In real amorphous materials HOMO’s and LUMO’s are usually associated with states *within* the gap and consequently their difference bears little resemblance to any experimentally meaningful value of a gap. Therefore it is important to devise alternative methods to determine optical gaps of amorphous networks.

**II. PREVIOUS WORK**

The experimental and theoretical activity prior to 1990 is well documented in a paper by Robertson where pertinent references can be found.<sup>7</sup> In this work Robertson reports his semiempirical tight-binding calculations for the optical gaps

and also reports several gaps for hydrogenated and nonhydrogenated  $a\text{-SiN}_x$  alloys.

Voskoboynikov *et al.*<sup>8</sup> studied experimentally some RDF's and optical gaps of silicon-rich silicon-nitrogen films as a function of the gas ratio, as early as 1976. It was then observed that the gaps increased as a function of the nitrogen content; the films seemed to contain hydrogen and large clusters of silicon. Their optical absorption curves already indicated pronounced tails for nitrogen-rich samples. Experimental radial distribution functions are scarce<sup>9</sup> and, to our knowledge, only total ones for the stoichiometric amorphous composition exist.<sup>10</sup> A Gaussian-based decomposition of the second peak of the total stoichiometric RDF into its partial contributions was carried out by Misawa *et al.* in Ref. 10. Electronic structure studies of  $a\text{-SiN}_x$ , in the range  $0 \leq x < 2$ , were performed by Kärcher *et al.*<sup>11</sup> using x-ray photoelectron spectroscopy where the valence band was thoroughly analyzed and the Si-N bonding was studied. It has now been established that the optical gap of  $a\text{-SiN}_x\text{:H}$  increases as  $x$  increases, slowly at first, and close to the stoichiometric compound,  $x=4/3=1.33$ , it attains its largest value.<sup>9</sup> There are some experimental results for the optical gap of nonhydrogenated amorphous silicon nitride reported by Sasaki *et al.*<sup>12</sup> and Davis *et al.*,<sup>9</sup> and the conclusions are similar.

Some theoretical efforts are based on the semiempirical tight-binding approach like those due to Robertson,<sup>7</sup> where optical gaps are calculated. Xanthakis *et al.*<sup>13</sup> look at a sample without gap states; they use a parametrized Kittler-Falicov method that draws upon parameters obtained by Robertson before 1990, and therefore less reliable. Bethe lattice calculations have been done by Martín-Moreno *et al.*<sup>14</sup> and by San-Fabián *et al.*<sup>15</sup> also using semiempirical parameters. Ordejón and Ynduráin<sup>16</sup> do nonparametrized calculations of  $a\text{-SiN}_x$  where the equilibrium positions of Si and N atoms in clusters are ported to the alloy network constructed *ad hoc*. They obtain a wealth of information including optical gaps; however, tetrahedral coordination of the silicon atoms and threefold planar coordination of the nitrogen atoms is *assumed* throughout, with interatomic distances of 2.33 Å for Si-Si and 1.74–1.76 Å for Si-N; compare to the crystalline values: 2.352 Å for Si-Si and 1.71–1.76 Å for Si-N.<sup>17</sup> A general characteristic of practically all calculations/simulations done up to date is that gap states, when considered, are introduced either by hand, progressively replacing Si by N, or by the algorithms that generate the random networks, *unlike* the procedure we have established. Recent semiempirical classical molecular-dynamics simulations by de Brito Mota *et al.*<sup>18</sup> produced structures whose total RDF's are the subject of comparison with ours and the point of departure for the study of the electronic properties of these alloys.<sup>5</sup> Since these RDF's do not closely agree with existing experiments, the structures might not be adequate to study their electronic structure. Densities of states, RDF's, and optical gaps for the crystalline and amorphous forms have also been reported by Ren and Ching,<sup>19</sup> Robertson<sup>20</sup> and Ferreira *et al.*<sup>21</sup>

Our recent work<sup>4</sup> has demonstrated that the application of *ab initio* techniques to the study of the atomic and electronic

structure of hydrogenated amorphous silicon,  $a\text{-Si:H}$ , and to the generation of random networks of C, Si, Ge, and silicon nitride using only 64-silicon atom cells is reasonable, despite the small number of atoms in the cell. No doubt, being able to handle a sample with more than 64 atoms would allow us to study larger defects such as voids, but nevertheless the results found are encouraging. We believe our success is due to two factors: first, we amorphize the cell at temperatures just below its melting point, thus avoiding the appearance of undesirable structures that are generated when samples are liquified first and solidified next; second, we use a quantum code based on the Harris functional that incorporates “quantum” forces as derivatives of the energy obtained. It is known<sup>22</sup> that the melting temperature of  $a\text{-Si}$  is 250 °C lower than the melting temperature of  $c\text{-Si}$  and therefore we expect it to be above the melting temperatures of the respective amorphous phases of all the alloys considered here by staying just below the melting temperatures of the crystalline counterparts. We now apply these *ab initio* methods to the generation of atomic random networks for 26 structures of  $a\text{-SiN}_x$  for 13 different nitrogen contents  $x$ , where  $0 \leq x \leq 1.29$ . These networks lead to RDF's in good agreement with what is known experimentally, and total and radial features are predicted for a variety of nitrogen contents. We also present an approach, similar to the experimental Tauc method,<sup>23</sup> to obtain optical gaps of amorphous materials based on *ab initio* calculations of the electron energy levels in the valence and conduction bands. The optical gaps obtained agree with existing experiments. This makes us reasonably optimistic that our method may be adequate for the understanding of atomic, electronic, and optical properties of other amorphous covalent materials and that it may stimulate further experimental and theoretical studies in the area.

### III. METHOD

The 26 amorphous samples of  $\text{SiN}_x$  were generated using FASTSTRUCTURE\_SIMANN<sup>24</sup> (FAST for short), a DFT molecular-dynamics code that is based on the Harris functional,<sup>25</sup> and optimization techniques with a fast force generator to allow simulated annealing/molecular-dynamics studies with quantum force calculations.<sup>26</sup> We use the local-density approximation parametrization due to Vosko, Wilk, and Nusair throughout.<sup>27</sup> The core is taken as full which means that an electron calculation is carried out, and a minimal basis set of atomic orbitals was chosen with a cutoff radius of 5 Å for the amorphization and 3 Å for the optimization. The physical masses of nitrogen and silicon are always used and this allows us to see realistic randomizing processes of the nitrogen atoms during the amorphization of the supercell. The default time step is given by  $\sqrt{m_{min}/5}$ , where  $m_{min}$  is the value of the smallest mass in the system (1.73 fs for this case); however, in order to better simulate the dynamical processes that occur in the amorphization, a time step of 6 fs was used throughout. The forces are calculated using rigorous formal derivatives of the expression for the energy in the Harris functional, as discussed by Lin and Harris.<sup>28</sup> For each atom, one function is used to represent the core part of the density and another to represent the valence

TABLE I. Contents, amorphization temperatures, densities and gaps for  $a$ -SiN $_x$ .

Sample	$x$	Amorph. temp. (K)	Density (g/cc)	Average gap (eV)
Si $_{64}$ N $_0$	0.000	1680	2.329	1.09
Si $_{59}$ N $_5$	0.085	1747	2.435	1.11
Si $_{54}$ N $_{10}$	0.185	1814	2.512	1.05
Si $_{49}$ N $_{15}$	0.306	1881	2.600	1.19
Si $_{44}$ N $_{20}$	0.455	1948	2.694	1.69
Si $_{39}$ N $_{25}$	0.641	2015	2.803	2.49
Si $_{34}$ N $_{30}$	0.882	2082	2.931	3.41
Si $_{33}$ N $_{31}$	0.939	2095	2.957	3.73
Si $_{32}$ N $_{32}$	1.000	2108	2.988	4.10
Si $_{31}$ N $_{33}$	1.065	2122	3.017	4.31
Si $_{30}$ N $_{34}$	1.133	2136	3.048	4.28
Si $_{29}$ N $_{35}$	1.207	2149	3.081	4.69
Si $_{28}$ N $_{36}$	1.286	2162	3.115	4.95

density. The types of orbital basis in FAST are *minimal* (consisting of the atomic orbitals occupied in the neutral atom; *sp*-valence type); *standard* (broadly equivalent to a Double Numeric basis set); and *enhanced* (broadly equivalent to a double numeric set together with polarization functions). The evaluation of the three-center integrals that contribute to the matrix elements in the one-particle Schrodinger equation is the time-limiting feature of FAST and each is performed using the weight-function method of Delley.<sup>29</sup>

In order to test the adequacy of the amorphous structures obtained with FAST we used it to calculate the size of the crystalline cell of  $\beta$ -Si $_3$ N $_4$  that minimizes the energy at the  $\Gamma$  point. The experimental crystalline volume is given by 145.920  $\text{\AA}^3$ ,<sup>30</sup> whereas the volume obtained in our calculation is 146.797  $\text{\AA}^3$ ; a deviation of only 0.6%. This makes us cautiously confident about the use of FAST to generate random networks of silicon-nitrogen alloys.

To avoid quenching from a melt, we amorphized the crystalline diamondlike structures, with a total of 64 atoms in the cell [(64- $y$ ) silicons,  $y$  randomly substituted nitrogens, and  $x = y/(64 - y)$ ] by heating them up, linearly, from room temperature to just below the corresponding melting point for each  $x$ , and then cooling them down to 0 K, Table I. To determine the melting temperatures for each concentration we linearly interpolated between pure silicon and the concentration of nitrogen in the stoichiometric compound, 57%, and then remained a few degrees below these values<sup>22</sup> (Table I). This then was followed by cycles of annealing and quenching at temperatures suggested by experiment and then the structures were energy optimized.

Since the 6 fs time step was kept constant for all runs and the amorphization temperatures increased with  $x$ , as indicated in Table I, the heating/cooling rates varied from  $2.30 \times 10^{15}$  K/s for pure silicon, to  $3.11 \times 10^{15}$  K/s for  $x = 1.29$ . The atoms were allowed to move within each cell, with periodic boundary conditions, whose volume was determined by the corresponding density and content, Table I. The densities were taken from the experimental results of Guraya

*et al.*<sup>9</sup> Once this first stage was completed, FAST was used to subject each cell to annealing cycles at 300 K with intermediate quenchings down to 0 K. Finally, the samples were energy optimized to make sure the final structures would have local energy minima.

To calculate the optical gaps we use the method described elsewhere.<sup>31</sup> The optical absorption coefficient  $\alpha$ , the fraction of energy lost by the wave on passing through a unit thickness of the material considered, for interband transitions is given by<sup>32</sup>

$$\alpha = (4\pi/n_o c)(2\pi e^2 \hbar^3 \Omega / m^2) \int \frac{N(E)N(E+\hbar\omega)|D|^2 dE}{\hbar\omega},$$

where  $D$  is the matrix element for transitions between states in different bands,  $\partial/\partial x$ , which will be taken to be the same as that for transitions between extended states in the same band,<sup>32</sup> (without the factor  $m/m^*$ ); i.e.,

$$D = \pi(a/\Omega)^{1/2},$$

where  $a$  is the average lattice spacing and  $\Omega$  is the volume of the specimen.

One characteristic feature of optical absorption in *amorphous* semiconductors is that certain selection rules, which exist for optically induced transitions in *crystalline* materials (particularly the conservation of  $k$ ), are relaxed.

For interband absorption in amorphous semiconductors the following assumptions are commonly made:<sup>32</sup>

(a) The matrix elements for the electronic transitions are constant over the range of photon energies of interest and given by  $D = \pi(a/\Omega)^{1/2}$ .

(b) The  $k$ -conservation selection rule is relaxed. As in Mott and Davis,<sup>32</sup> we take the matrix element to be the same whether or not either the initial or final state, or both, are localized.

Under these conditions the optical absorption coefficient  $\alpha$ , for interband transitions, is given by

$$\alpha = \frac{8\pi^4 e^2 \hbar^2 a}{n_o c m^2 \omega} \int N_V(E)N_C(E+\hbar\omega) dE,$$

where the integration is over all pairs of states in the valence and conduction bands separated by an energy  $\hbar\omega$ .  $n_o$  is the refractive index, assumed to be independent of energy.<sup>32</sup>

For amorphous tetravalent semiconductors this leads to the well-known relationship  $\sqrt{\alpha(\omega)\hbar\omega} = \text{const}(\hbar\omega - E_0)$  obtained by Tauc<sup>23</sup> under the assumption of parabolic bands. This formula has been used extensively by experimentalists to obtain the optical gap  $E_0$  by fitting a straight line to the low-energy end of the data, plotted as  $\sqrt{\alpha(\omega)\hbar\omega}$  vs  $(\hbar\omega - E_0)$ , and looking at the intersection of this line with the horizontal axis  $(\hbar\omega - E_0)$ .

Since  $\alpha$  is proportional to the fraction of energy lost by the wave on passing through the material, this implies that it is proportional to the number of electronic transitions that go from the valence to the conduction band,  $N_t(\hbar\omega)$ . Therefore plotting  $\sqrt{N_t(\hbar\omega)\hbar\omega}$ , instead of  $\sqrt{\alpha(\omega)\hbar\omega}$ , should give the same type of behavior as experimentally observed although with a different slope; however, the intersection with the

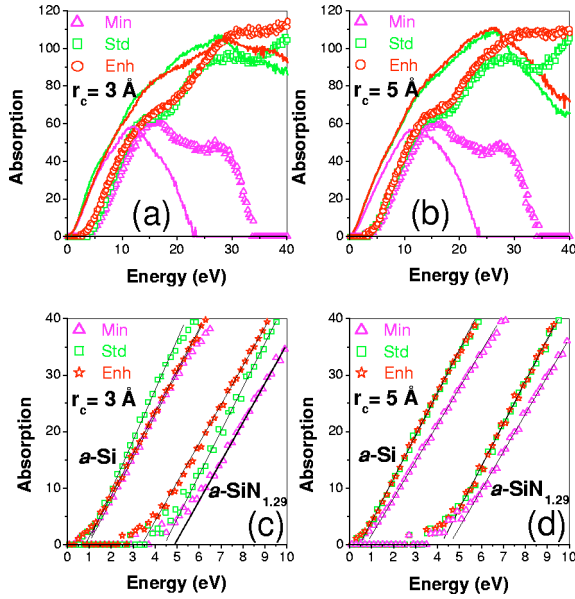


FIG. 1. (Color online) Optical absorption curves for *minimal*, *standard*, and *enhanced* orbital sets for one of the two runs. The cutoff radius is 3 Å for (a) and (c) and 5 Å for (b) and (d). In (a) and (b) the symbols refer to  $a\text{-SiN}_{1.29}$  and the lines to  $a\text{-Si}$ .

horizontal  $\hbar\omega$  axis, the optical gap  $E_0$ , remains unaltered. This is precisely what we do. To find the optical gap we look at the intersection of the linear fits to the low-energy end of the absorption curves, the  $\sqrt{N_f(\hbar\omega)\hbar\omega}$  data. The linear fits are carried out as follows: we look at the low-energy region of the absorption spectrum,  $0 \leq \hbar\omega \leq 10$  eV and fit it with a straight line, choosing the line that gives the best linear fit for the largest number of points. The errors estimated for the slopes of these linear fits are smaller for the purer samples and increase due to the presence of states within the gap for high nitrogen contents. For example, for pure silicon the slope is  $7.496 \pm 0.251$  and for the nearly stoichiometric sample  $7.102 \pm 1.11$ .

Both the cutoff radius<sup>33</sup> and the completeness of the orbital set<sup>34</sup> play a role in simulations. To test this we calculated the energy levels at the  $\Gamma$  point using the three orbital sets of FAST: *minimal*, *standard*, and *enhanced* for two cutoff radii 3 Å and 5 Å and plotted  $\sqrt{N_f(\hbar\omega)\hbar\omega}$  for the three sets. Figure 1(a) depicts the results for one of the two runs, both for pure  $a\text{-Si}$  and for  $a\text{-Si}_3\text{N}_4$  using  $r_c = 3$  Å; Fig. 1(b) depicts the same information but now for  $r_c = 5$  Å; the lines are for pure silicon whereas the symbols refer to silicon nitride. The shoulders observed for the silicon nitride curves at about 30 eV are due to transitions from the nitrogen  $s$ -like band to the conduction band. The way optical gaps are obtained is illustrated in Figs. 1(c) and 1(d) where the linear fits can be appreciated. The combination that best describes the experimental results is the *minimal* set with a cutoff radii of 3 Å; this cutoff should be compared to those used by Sankey *et al.*<sup>33</sup> of  $\approx 2.6$  Å.

#### IV. RESULTS AND DISCUSSION

It should be kept in mind that our objective is to generate realistic amorphous structures of  $a\text{-SiN}_x$  and not, in any way,

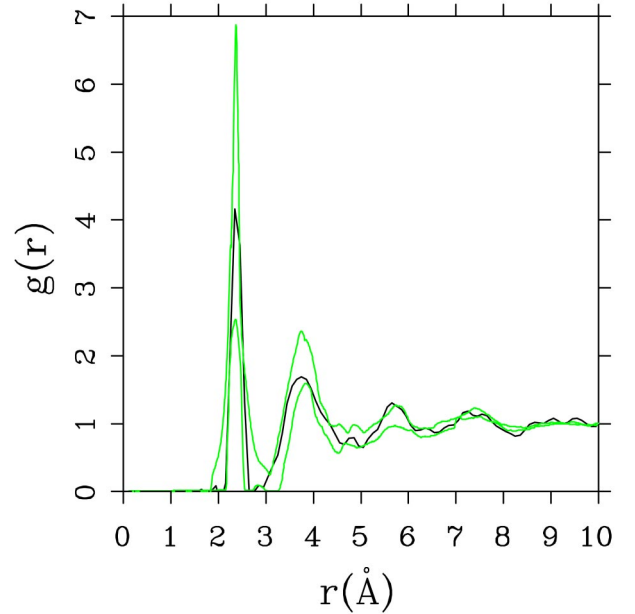


FIG. 2. (Color online) Radial distribution function for pure silicon with a 6 fs time step. The light curves are the upper and lower experimental bounds (Ref. 4).

to mimic the experimental processes used to produce these alloys. The atomic topology determines the electronic properties of the amorphous samples and therefore, any understanding of the RDF's and the atomic distribution in the random networks is relevant for the characterization of the electronic and optical properties of these materials.

We performed two runs for each  $x$  value, and from  $x = 0.88$  on ( $a\text{-Si}_{34}\text{N}_{30}$ ) the number of nitrogens was increased one at a time to be able to map the interesting processes that occur for these contents (percolation of the Si-Si bonds, widening of the optical gaps, etc). The total and partial RDF's and the optical gaps of each of the 26 runs are calculated and averaged by corresponding pairs. In Fig. 2 we present the total RDF for an amorphous structure of pure silicon constructed with a 6 fs time step; the light curves are the upper and lower experimental bounds obtained from a previous work.<sup>4</sup> It can be seen that our simulations agree very well with the experiment since our RDF falls within these bounds and the four experimental radial peaks are reproduced very nicely.

All total and partial RDF's for each of the 12 nonzero values of  $x$  are given in Fig. 3, since this is the experimental information most frequently determined. The variation of the partial RDF's for Si-Si, Si-N, and N-N as a function of content, and their contribution to the total RDF, is shown. As the nitrogen content increases the first peak of the total RDF (1.85 Å), which is due to the Si-N average nearest-neighbor contributions,  $\langle nn \rangle$ , increases systematically and the  $\langle nn \rangle$  Si-Si peak (2.45 Å) decreases systematically. The third peak of the total RDF's moves toward lower  $r$ , 3.25 Å to 2.95 Å, as  $x$  increases since the N-N contribution becomes more predominant for high content. In our structures there are no  $\langle nn \rangle$  nitrogens since the content is below stoichiometry and nitrogens have a marked tendency to bind to silicons. No

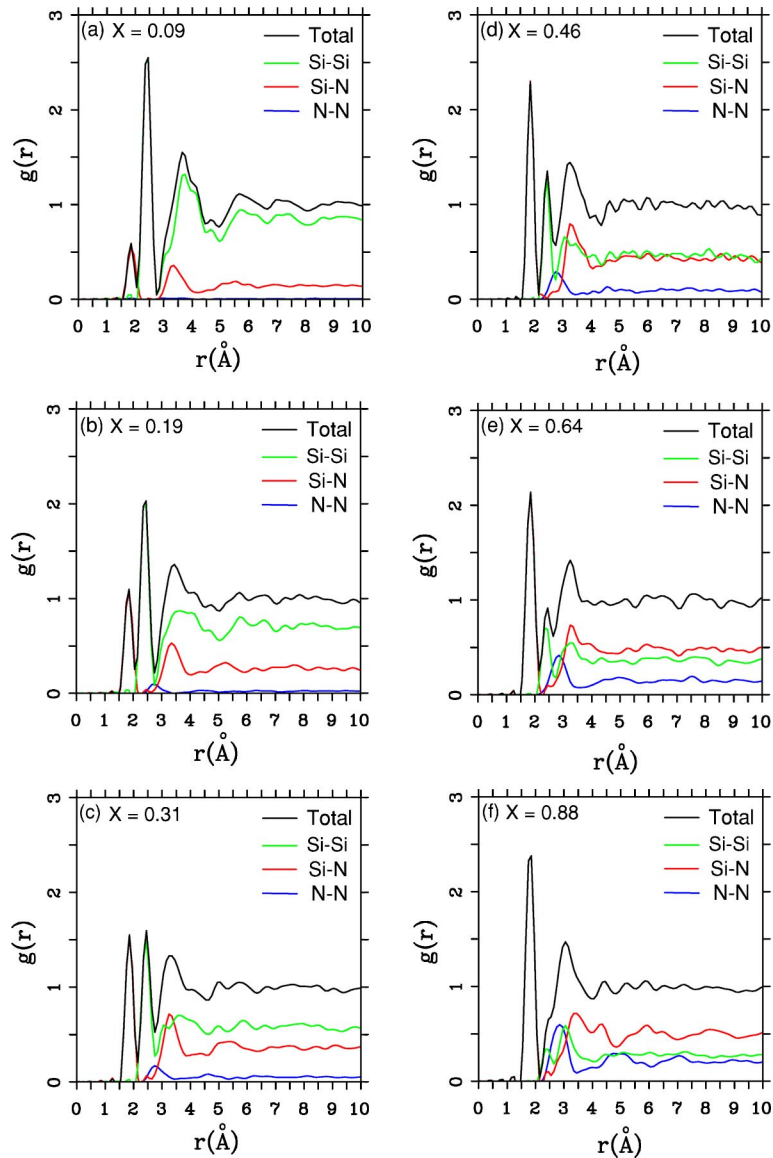


FIG. 3. (Color online) Total and partial RDF's for  $a\text{-SiN}_x$ . (a)  $x=0.09$ , (b)  $x=0.19$ , (c)  $x=0.31$ , (d)  $x=0.46$ , (e)  $x=0.64$ , (f)  $x=0.88$ , (g)  $x=0.94$ , (h)  $x=1.00$ , (i)  $x=1.07$ , (j)  $x=1.13$ , (k)  $x=1.21$ , and (l)  $x=1.29$ .

nitrogen molecules are formed even though for  $x > 1$  the starting diamond structure *does* contain nearest-neighbor nitrogens. For the nearly stoichiometric sample,  $x = 1.29$ , Fig. 3(l), the Si-Si  $\langle nn \rangle$  contribution to the total RDF has practically disappeared and this implies that there is a nitrogen atom between every pair of silicons indicating a tendency to form 6-atom closed rings, Si-N-Si-N-Si-N, typical of the  $\text{Si}_3\text{N}_4$  structures. The growth of the Si-N peak as nitrogen increases bears out this behavior. This is also borne out by the results presented in Fig. 4 where a study of the average coordination numbers  $\langle cn \rangle$  in the 13 random networks is depicted. The following cutoff radii were used: Si-Si, 2.55 Å; N-N, 3.35 Å; and Si-N, 2.15 Å, which are the positions of the minima after the first peaks of the corresponding partials. Figure 4(a) shows the results of our simulations and it can be seen that the N-N plot flattens for  $x \approx 1.1$ , the percolation threshold of Si-Si bonds;<sup>35</sup> the Si-Si  $\langle nn \rangle$  go from 4 to practically 0. The Si-N graph refers to the  $\langle nn \rangle$

nitrogens around the silicon atoms and varies from zero to four, whereas the N-Si refers to the  $\langle nn \rangle$  silicons around nitrogens and indicates that nitrogens immediately surround themselves with practically three Si, saturating its valence.

The crossing of the Si-Si and Si-N plots at  $x \approx 0.7$  is in agreement with experiment (Davis *et al.*<sup>9</sup>). There is a crossing of the Si-Si, N-Si, and N-N plots at  $x \approx 0.3$  and a crossing of N-Si and Si-N at  $x \approx 1.0$  which have been observed experimentally for *hydrogenated* alloys by Guraya *et al.*,<sup>9</sup> Fig. 4(b). However, due to the presence of hydrogen a curvature appears in the  $\langle cn \rangle$  for Si-Si, Si-N, and N-Si so, in order to compare our results to this experiment, we did the following. We carried out the sum of N-H and N-Si from the experiment, the average total number of atoms that surround a N, N-\*, and plotted it along with our N-Si. We also did the sum of the experimental Si-N, Si-Si, and Si-H, the average total number of atoms that surround a Si, Si-\*, and plotted that along with our sum of Si-N plus Si-Si. This is presented in

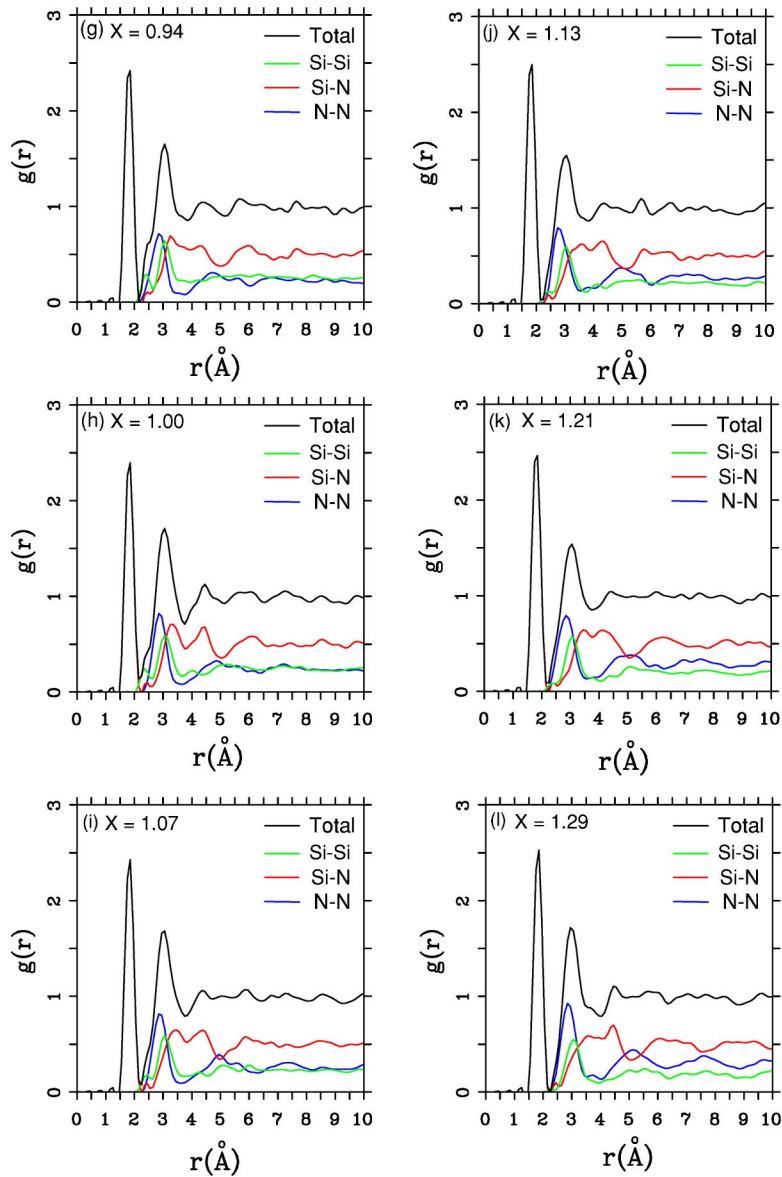


FIG. 3. (Continued).

Fig. 4(c). It is clear that our predictions closely agree with the integrated experimental results and show that our structures are realistic. The discrepancies are most likely due to existing dangling and floating bonds. Our stoichiometric sample does not have voids because the coordination numbers observed are close to 3 for nitrogen, 4 for silicon, and 0 for Si-Si. It would also be difficult to observe large voids in a 64-atom sample.

The curves of Fig. 3 are plotted as they are, i.e., as the number of atoms at a certain radial distance from a given one. In order to compare with x-ray-or neutron-diffraction experiments the corresponding weights should be calculated and applied to the partial contributions and then summed to give the total RDF's; this we do for the stoichiometric sample where some experimental results have been reported. The composition of the second peak of the total RDF for this sample is given in Fig. 3(l) and it can be observed that it

agrees *qualitatively* with the experiment, Misawa *et al.* in Ref. 10, since it is formed by the average second neighbor,  $\langle 2n \rangle$ , contributions of mainly the N-N and Si-Si partials and to a lesser extent by the Si-N partial.<sup>36</sup> The third peak is essentially due to the Si-N partial with a small contribution from the N-N partial. In order to *quantitatively* compare our predictions with the few available experiments we calculated the structure of the second peak of the nearly stoichiometric cell considering whether the radial features were determined using x rays or neutrons. To do so, one needs to use the expression quoted by Aiyama *et al.*:<sup>10</sup>

$$g(r) = \frac{c_1^2 f_1^2}{\langle f \rangle^2} g_{11}(r) + \frac{2c_1 c_2 f_1 f_2}{\langle f \rangle^2} g_{12}(r) + \frac{c_2^2 f_2^2}{\langle f \rangle^2} g_{22}(r),$$

where  $c_1$  is the ratio of the number of Si atoms to the total number of atoms and  $c_2$  the ratio of N atoms to the total

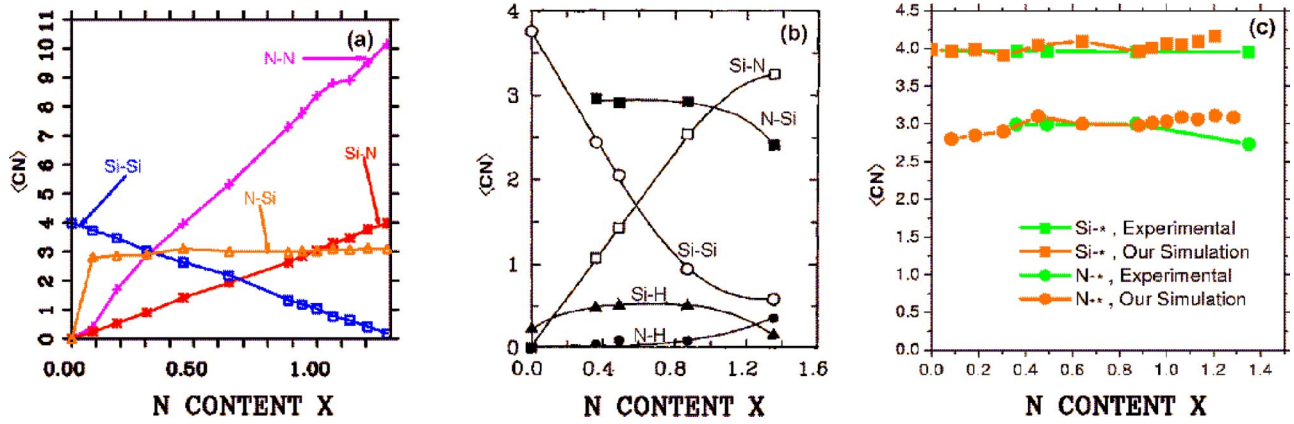


FIG. 4. (Color online) Average coordination numbers  $\langle cn \rangle$  as a function of  $x$ . (a) Our results. (b) Experimental results for hydrogenated alloys from Guraya *et al.* (c) Comparison of the integrated results (see text). Lines are drawn as guides to the eye.

number.  $f_1$  is the Si structure factor for x-ray scattering, or the scattering amplitude for neutron scattering, and correspondingly  $f_2$  is for N.  $g_{ij}(r)$  are the partial pair distribution functions,  $g_{11} = g_{SiSi}$ , etc. Finally,  $\langle f \rangle^2 = (\sum_{i=1}^2 c_i f_i)^2$ .

Figure 5 shows the experimental and simulated results and the quantitative agreement is excellent even though the experimentalists only used Gaussian fits to simulate the structure of the second peak. It is understandable that silicons are more prominent for x rays than for neutrons, and the opposite occurs for nitrogens. That is why  $[(c_{Si}^2 f_{Si}^2) / \langle f \rangle^2] g_{SiSi}(r)$  is more prominent for the x-ray simulation and  $[(c_N^2 f_N^2) / \langle f \rangle^2] g_{NN}(r)$  is more prominent for the neutron simulation. For this peak x rays show a shift of the total RDF toward higher values of  $r$  which is reproduced in our simulations.

Figure 6 is the comparison of our *ab initio* results with the classical Monte Carlo simulations of de Brito Mota *et al.*<sup>18</sup> who used empirical potentials developed *a la* Tersoff for the interactions between Si and N. It is clear that although the positions of some peaks are reproduced in both simulations, the general behavior of the total RDF's only agrees qualitatively at best. Comparison of the two simulational results with experiment for the stoichiometric samples is also presented in this figure, where agreements and discrepancies can be appreciated.

For the optical gaps we first calculated the electronic energy levels of the valence and conduction bands at the  $\Gamma$  point with FAST to obtain  $\alpha$ , the optical absorption coefficient. We then performed the Tauc-like approach described before. This theoretical Tauc-like procedure bypasses completely the gap states and therefore ignores the nature of these states leading to gap values comparable to experiment.

Looking at the electronic structure of amorphous cells with 64 atoms at the  $\Gamma$  point is a well-known procedure in the field. However it must be kept in mind that the larger the cell and the larger the number of atoms in the cell the better the approximation becomes. Here again the main obstacles are the computational resources needed to deal with larger cells.

The slope of our Tauc fit diminishes first and increases afterwards, as experimentally reported by Hasegawa *et al.*<sup>9</sup> (Fig. 7, right vertical axis, square symbols). In order to com-

pare experiment and simulation we have plotted the average slope, which is the average of the two corresponding values of each of the two runs, as a function of the energy gap using a vertical coordinate given by  $\sqrt{N_I}(\hbar\omega)\hbar\omega/\hbar\omega$  (Fig. 8, left vertical axis, triangle symbols). The experimental results, right vertical axis, that Hasegawa and co-workers report, is given in units of  $10^5 \text{ eV}^{-1} \text{ cm}^{-1}$ , so the most we can hope for is the qualitative comparison of both results given in Fig. 7. The similarity is quite impressive, even though the experimental results are for hydrogenated *a*-SiN<sub>x</sub> samples, indicating that our approach seems to be along the right lines for amorphous covalent alloys as well.

In Fig. 8 we plot the optical gaps of several experimental and theoretical results reported in the literature.<sup>31</sup> The experimental hydrogenated results are due to Hasegawa *et al.*<sup>9</sup> and Guraya *et al.*<sup>9</sup> The experimental nonhydrogenated gaps are due to Sasaki *et al.*<sup>12</sup> and Davis *et al.*<sup>9</sup> The simulations of

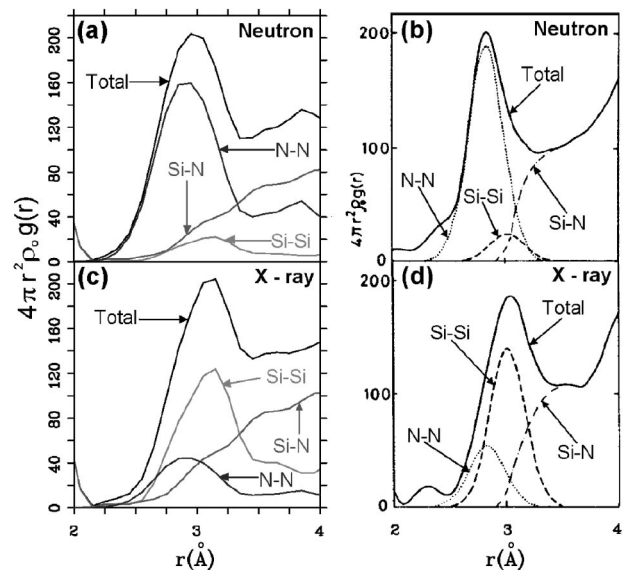


FIG. 5. Comparison of the simulated (a) and (c), and experimental (b) and (d), structures of the second peak of the nearly stoichiometric sample when x rays and neutrons are used, respectively. X rays show a shift toward higher values of  $r$  for this peak, which is reproduced in our simulations.

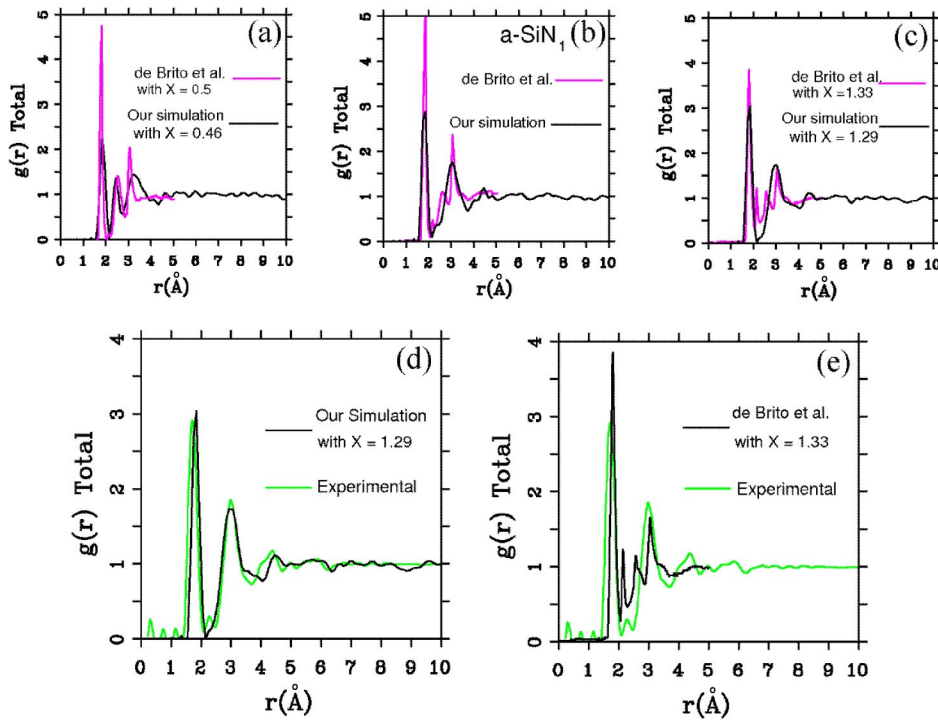


FIG. 6. (Color online) Comparison of our results and those obtained by de Brito Mota *et al.* (Ref. 18) for the total RDF. The agreement is at best qualitative although the position of some of the peaks coincide for the samples (a)–(c). The experimental total FDR (Ref. 10) is compared to (d) our simulations, and (e) to de Brito Mota’s simulations.

Ordejón *et al.*<sup>16</sup> for samples without hydrogen, an atomistic calculation with adjusted parameters, are also included. The optical gaps, calculated using our approach, are of the correct order of magnitude and behave very similar to experiment. Our gaps are below all results for  $x \leq 0.5$  and above all results for  $x \geq 0.6$ . For  $x \approx 1.3$  experiment and simulation become indistinguishable; the behavior clearly changes for  $x \approx 1.1$ , the percolation threshold of Si-Si bonds mentioned above.<sup>35</sup>

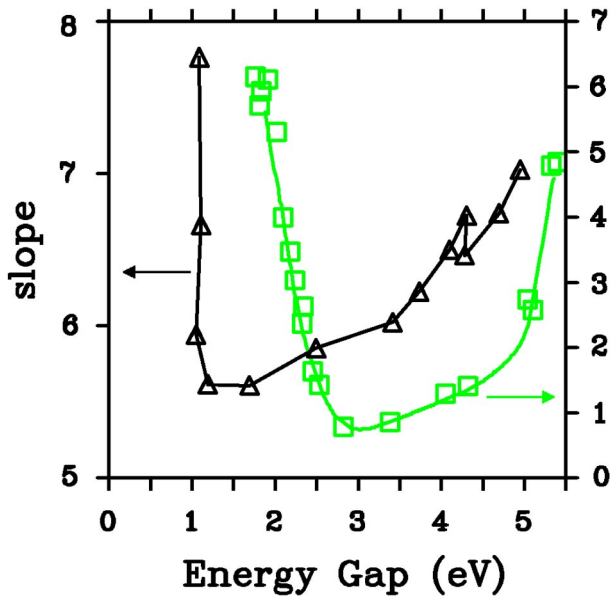


FIG. 7. (Color online) Behavior of the Tauc *slope* as a function of  $x$ . The right vertical axis, square symbols, are the experimental results due to Hasegawa *et al.* (Ref. 9) for glow discharge  $a\text{-SiN}_x\text{:H}$ . The left vertical axis, triangle symbols, are our results using the Tauc-like approach.

V. CONCLUSIONS

We have devised an *ab initio* process to generate amorphous networks of  $\text{SiN}_x$  alloys ( $0 \leq x \leq 1.29$ ) that lead to atomic topologies in agreement with the existing experimental results. The atomic structures have total RDF’s and average coordination numbers that agree with the scarce experimental results. The simulated partial RDF’s show that the Si-Si  $\langle nn \rangle$  peak disappears as nitrogen increases indicating a tendency to form 6-atom arrangements as the content  $x$  ap-

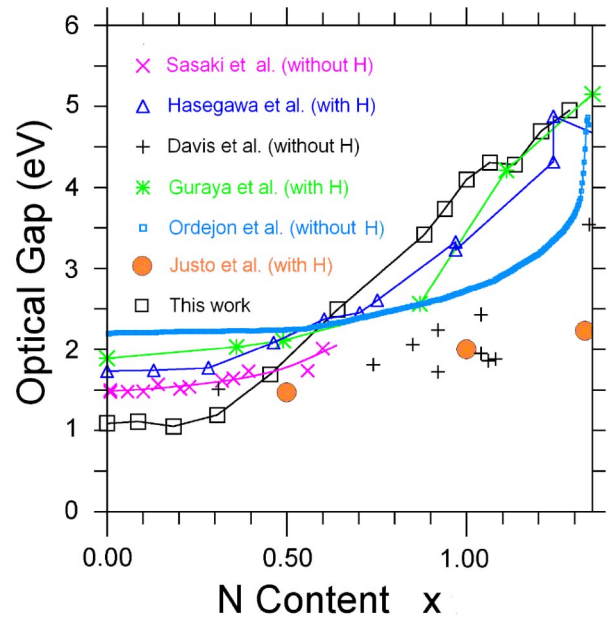


FIG. 8. (Color online) Experimental and calculated optical gaps for amorphous alloys of silicon-nitrogen for various contents  $x$  (see text) (Ref. 31). Lines are drawn as guides to the eye.

proaches the stoichiometric value. Experiment shows that for  $\alpha$ -Si<sub>3</sub>N<sub>4</sub>, Si, and N form 6-atom closed rings, Si-N-Si-N-Si-N, typical of the crystalline Si<sub>3</sub>N<sub>4</sub> structures. The growth of the Si-N peak as nitrogen increases bears this out. No nitrogen-nitrogen bonds, including molecular nitrogen, are observed in the final structures even though for  $x > 1$  the starting diamond structure *does* contain nitrogens next to one another. For  $x \approx 1.1$  the effects of the percolation threshold of the Si-Si bonds is observed in the N-N  $\langle 2n \rangle$  and in the optical gaps. For  $x \approx 0.7$  the Si-Si and Si-N neighbors are practically the same, as found experimentally. Also, Si-Si, N-Si, and N-N are practically the same for  $x \approx 0.3$  as are Si-N and N-Si for  $x \approx 1.0$ . The integrated experimental results and our simulations agree. The first prominent peak in the total RDF of the nearly stoichiometric sample is due to Si-N and an analysis of the second peak indicates that N-N, Si-Si, and Si-N contribute to it, in quantitative agreement with experiment. The third peak is mainly due to the Si-N, with a small contribution from the N-N; no experimental results exist for comparison. We report *all* partials and totals for the contents studied.

We have also devised an optical Tauc-like approach to calculate optical absorption curves and optical gaps of amorphous materials that give values in agreement with experi-

ment. The optical gaps were obtained by a Tauc-like approach applied to all the electronic transitions that can occur between the valence and conduction states, using the assumptions of Mott and Davis,<sup>32</sup> and we found that the  $\sqrt{N_i(\hbar\omega)\hbar\omega}$  vs  $(\hbar\omega - E_0)$  plots are very similar to the ones reported experimentally for amorphous tetravalent semiconductors. In particular we calculated the variation of the slope of our Tauc-like fits to the low-energy end of the optical absorption curves and this behavior agrees with what has been experimentally reported by Hasegawa and co-workers on glow discharge  $\alpha$ -SiN<sub>x</sub>:H.<sup>9</sup>

Our approach, being *ab initio*, is of wider applicability than classical or semiempirical ones and may be relevant for the understanding of the physics of amorphous covalent materials.

#### ACKNOWLEDGMENTS

A.A.V. thanks DGAPA-UNAM for financing Projects Nos. IN101798 and IN100500. F.A. acknowledges CONA-CyT for supporting his Ph.D. studies. This work was carried out on an Origin 2000 computer provided by DGSCA, UNAM.

\*Electronic address: valladar@servidor.unam.mx

<sup>1</sup>J.M. Holender and G.J. Morgan, *J. Phys.: Condens. Matter* **3**, 7241 (1991).

<sup>2</sup>P. Walsh, A. Omeltchenko, R.K. Kalia, A. Nakano, P. Vashishta, and S. Saini, *Appl. Phys. Lett.* **82**, 118 (2003).

<sup>3</sup>A. Horsfield and S.D. Kenny, in *Tight-Binding Approach to Computational Materials Science*, edited by P.E.A. Turchi, A. Gonis, and L. Colombo, Mater. Res. Soc. Symp. Proc. 491 (Materials Research Society, Pittsburgh, 1998).

<sup>4</sup>A.A. Valladares, F. Alvarez, Z. Liu, J. Stitch, and J. Harris, *Eur. Phys. J. B* **22**, 443 (2001); F. Alvarez, C.C. Díaz, Ariel A. Valladares, and R.M. Valladares, *Phys. Rev. B* **65**, 113108 (2002).

<sup>5</sup>J.F. Justo, F. de Brito Mota, and A. Fazzio, *Phys. Rev. B* **65**, 073202 (2002).

<sup>6</sup>See, for instance, V. Olevano, S. Albrecht, and L. Reining, in *The Optical Properties of Materials*, edited by E.L. Shirley, J.R. Chelikowsky, S.G. Louie, and G. Martínez, Mater. Res. Soc. Symp. Proc. 579 (Materials Research Society, Pittsburgh, 2001).

<sup>7</sup>J. Robertson, *Philos. Mag. B* **63**, 47 (1991).

<sup>8</sup>V.V. Voskoboynikov, V.A. Gritsenko, N.D. Dikovskaya, B.N. Saitsev, K.P. Mogilnicov, V.M. Osadchii, S.P. Sinitisa, and F.L. Edelman, *Thin Solid Films* **32**, 339 (1976).

<sup>9</sup>S. Hasegawa, M. Matuura, and Y. Kurata, *Appl. Phys. Lett.* **49**, 1272 (1986); E.A. Davis, N. Piggins, and S.C. Bayliss, *J. Phys. C* **20**, 4415 (1987); M.M. Guraya, H. Ascolani, G. Zampieri, J.I. Cisneros, J.H. Dias da Silva, and M.P. Cantão, *Phys. Rev. B* **42**, 5677 (1990); G. Santana and A. Morales-Acevedo, *Sol. Energy Mater. Sol. Cells* **60**, 135 (2000).

<sup>10</sup>T. Aiyama, T. Fukunaga, K. Niihara, T. Hirai, and K. Suzuki, *J. Non-Cryst. Solids* **33**, 131 (1979); M. Misawa, T. Fukunaga, K. Niihara, T. Hirai, and K. Suzuki, *ibid.* **34**, 313 (1979); T. Fukunaga, T. Goto, M. Misawa, T. Hirai, and K. Suzuki, *ibid.* **95&96**, 1119 (1987).

<sup>11</sup>R. Kärcher, L. Ley, and R.L. Johnson, *Phys. Rev. B* **30**, 1896 (1984).

<sup>12</sup>G. Sasaki, M. Kondo, S. Fujita, and A. Sasaki, *Jpn. J. Appl. Phys.*, Part 1 **21**, 1394 (1982).

<sup>13</sup>J.P. Xanthakis, S. Papadopoulos, and P.R. Mason, *J. Phys. C* **21**, L555 (1988).

<sup>14</sup>L. Martín-Moreno, E. Martínez, J.A. Vergés, and F. Ynduráin, *Phys. Rev. B* **35**, 9683 (1987).

<sup>15</sup>E. San-Fabián, E. Louis, L. Martín-Moreno, and J.A. Vergés, *Phys. Rev. B* **39**, 1844 (1989).

<sup>16</sup>P. Ordejón and F. Ynduráin, *J. Non-Cryst. Solids* **137&138**, 891 (1991).

<sup>17</sup>O. Borgen and H.M. Seip, *Acta Chem. Scand.* **15**, 1789 (1961).

<sup>18</sup>F. de Brito Mota, J.F. Justo, and A. Fazzio, *Phys. Rev. B* **58**, 8323 (1998); *Int. J. Quantum Chem.* **70**, 973 (1998); *J. Appl. Phys.* **86**, 1843 (1999); J.F. Justo, F. de Brito Mota, and A. Fazzio, *Mater. Res. Soc. Symp. Proc.* **538**, 555 (1999).

<sup>19</sup>S.Y. Ren and W.Y. Ching, *Phys. Rev. B* **23**, 5454 (1981).

<sup>20</sup>J. Robertson, *Philos. Mag. B* **44**, 215 (1981); *J. Appl. Phys.* **54**, 4490 (1983); *J. Robertson, Philos. Mag. B* **63**, 44 (1991); *J. Robertson and M.J. Powell, Appl. Phys. Lett.* **44**, 415 (1984).

<sup>21</sup>E.C. Ferreira and C.E.T. Gonçalves da Silva, *Phys. Rev. B* **32**, 8332 (1985).

<sup>22</sup>J.M. Poate, in *Electronic Materials. A New Era in Materials Science*, edited by J.R. Chelikowsky and A. Franciosi (Springer-Verlag, Berlin, Heidelberg, 1991), p. 323.

<sup>23</sup>J. Tauc, in *Optical Properties of Solids*, edited by F. Abele (North Holland, Amsterdam, 1970).

<sup>24</sup>FASTSTRUCTURE\_SIMANN, User Guide, Release 4.0.0 (Molecular Simulations, San Diego, 1996).

<sup>25</sup>J. Harris, *Phys. Rev. B* **31**, 1770 (1985).

<sup>26</sup>Xiao-Ping Li, J. Andzelm, J. Harris, and A.M. Chaka, in *Chemical Applications of Density-Functional Theory*, edited by B.B.

- Laird, R.B. Ross, and T. Ziegler (American Chemical Society, Washington, DC, 1996), Chap. 26.
- <sup>27</sup>S.H. Vosko, L. Wilk, and M. Nusair, *Can. J. Phys.* **58**, 1200 (1980).
- <sup>28</sup>Z. Lin and J. Harris, *J. Phys.: Condens. Matter* **5**, 1055 (1992).
- <sup>29</sup>B. Delley, *J. Chem. Phys.* **92**, 508 (1990).
- <sup>30</sup>S. Wild, P. Grieveson, and K.H. Jack, *Fourth Symposium on Special Ceramics*, British Ceram. Res. Assoc. **1968**, 237 (1968).
- <sup>31</sup>Fernando Alvarez and Ariel A. Valladares, *Appl. Phys. Lett.* **80**, 58 (2002).
- <sup>32</sup>N.F. Mott and E.A. Davis, *Electronic Processes in Non-Crystalline Materials* (Oxford University Press, Oxford, 1971), p. 238.
- <sup>33</sup>O.F. Sankey and D.J. Niklewsky, *Phys. Rev. B* **40**, 3979 (1989).
- <sup>34</sup>Steven Louie (private communication).
- <sup>35</sup>E. Martínez and F. Ynduráin, *Phys. Rev. B* **24**, 5718 (1981).
- <sup>36</sup>Fernando Alvarez and Ariel A. Valladares, *Rev. Mex. Fis.* **48**, 528 (2002).